12-29-2021

Vapor isotopic evidence for the worsening of winter air quality by anthropogenic combustion-derived water

Meng Xing
Chinese Academy of Sciences

Weiguo Liu
Chinese Academy of Sciences

Xia Li
Chinese Academy of Sciences

Weijian Zhou
Chinese Academy of Sciences

Qiyuan Wang
Chinese Academy of Sciences

See next page for additional authors

Recommended Citation

Xing, M., Liu, W., Li, X., Zhou, W., Wang, Q., Tian, J., Li, X., Tie, X., Li, G., Cao, J., Bao, H., & An, Z. (2021). Vapor isotopic evidence for the worsening of winter air quality by anthropogenic combustion-derived water. *Proceedings of the National Academy of Sciences of the United States of America, 117* (52), 33005-33010. https://doi.org/10.1073/PNAS.1922840117

Vapor isotopic evidence for the worsening of winter air quality by anthropogenic combustion-derived water

Meng Xing[a,b], Weiguo Liu[a,b], Xia Li[a,c], Weijian Zhou[a,b,d], Qiyuan Wang[a,b,c], Jie Tian[a,b,c], Xiaofei Li[a,b,c], Xuexi Tie[a,b,c], Guohui Li[a,b,c], Junji Cao[a,b,c,e,f,1], Huiming Bao[g,h,1], and Zhisheng An[a,b,d,e,1]

[a]State Key Laboratory of Loess and Quaternary Geology, Institute of Earth Environment, Chinese Academy of Sciences, 710061 Xi'an, China; [b]Center for Excellence in Quaternary Science and Global Change, Chinese Academy of Sciences, 710061 Xi'an, China; [c]Key Laboratory of Aerosol Chemistry and Physics, Institute of Earth Environment, Chinese Academy of Sciences, 710061 Xi'an, China; [d]Interdisciplinary Research Center of Earth Science Frontier, Beijing Normal University, 100875 Beijing, China; [e]Open Studio for Oceanic-Continental Climate and Environment Changes, Qingdao National Laboratory for Marine Science and Technology, Qingdao, China; [f]Department of Earth and Environmental Sciences, Xi'an Jiaotong University, 710049 Xi'an, China; [g]International Center for Isotope Effects Research, School of Earth Science and Engineering, Nanjing University, 210023 Nanjing, China; and [h]Department of Geology and Geophysics, Louisiana State University, Baton Rouge, LA 70803

Contributed by Zhisheng An, November 5, 2020 (sent for review December 30, 2019; reviewed by Gabriel J. Bowen and Xin Yang)

Anthropogenic combustion-derived water (CDW) may accumulate in an airshed due to stagnant air, which may further enhance the formation of secondary aerosols and worsen air quality. Here we collected three-winter-season, hourly resolution, water-vapor stable H and O isotope compositions together with atmospheric physical and chemical data from the city of Xi'an, located in the Guanzhong Basin (GZB) in northwestern China, to elucidate the role of CDW in particulate pollution. Based on our experimentally determined water vapor isotope composition of the CDW for individual and weighted fuels in the basin, we found that CDW constitutes 6.2% of the atmospheric moisture on average and its fraction is positively correlated with [$PM_{2.5}$] (concentration of particulate matter with an aerodynamic diameter less than 2.5 μm) as well as relative humidity during the periods of rising [$PM_{2.5}$]. Our modeling results showed that CDW added additional average 4.6 μg m^{-3} $PM_{2.5}$ during severely polluted conditions in the GZB, which corresponded to an average 5.1% of local anthropogenic [$PM_{2.5}$] (average at ∼91.0 μg m^{-3}). Our result is consistent with the proposed positive feedback between the relative humidity and a moisture sensitive air-pollution condition, alerting to the nontrivial role of CDW when considering change of energy structure such as a massive coal-to-gas switch in household heating in winter.

water vapor isotopes | WRF-Chem simulation | air quality | winter haze

An estimated 3 million people are killed each year owing to outdoor air pollution (1). Overall mean mortality rate increases ∼1.2% with each 10 μg m^{-3} increase in [$PM_{2.5}$] (concentration of particulate matter with an aerodynamic diameter less than 2.5 μm) (2). Considering a close relationship between air pollution and energy structure (3, 4), countries facing severe air pollution have been adjusting their energy structure to improve air quality. In the past several years, China has invested heavily in reducing air pollution in major cities (5), and there has been a significant decrease in annual [$PM_{2.5}$] since 2013 (6). Despite many drastic efforts, haze events, correlated with high [$PM_{2.5}$], still occur frequently, especially in cities on the North China Plain (7, 8). In the heavily polluted Beijing-Tianjin-Hebei region, a series of regulatory policies has been implemented (5, 9), including using natural gas instead of coal (10, 11). Since 2015, a large-scale project of coal-to-gas switch has been deployed in urban and rural areas in China (12, 13).

It has been proposed that in northern China, severe haze is the synergetic effect of the interactions between anthropogenic emissions and atmospheric processes (7). Among the many causes of haze events, atmospheric water vapor or specifically relative humidity (RH) enhances the rate of heterogeneous oxidation of SO_2 and NO_X and in turn exerts a positive feedback on the rising of [$PM_{2.5}$] (14–17). Water vapor in the planetary boundary layer (PBL) comes mostly from the oceans via evaporation and transport or from continental water via evapotranspiration (18, 19). Combustion-derived water (CDW), a source of water vapor coming from fossil fuel or biomass burning, is negligible in the global atmospheric water budget. However, Gorski et al. (20) reported up to 13% of the water vapor in PBL was from CDW during certain days in Salt Lake City, Utah, located in an enclosed basin in northern America. This is a significant water contribution and should be verified independently in similar urban environments. The increased CDW fraction in air moisture could simply be a passive result of multiday accumulation in a polluted/stagnant PBL. Or, the CDW added to an airshed during polluted days could accelerate the formation of secondary aerosols, further stabilize the PBL, and reinforce CDW accumulation (15, 20). Pinning the exact role of CDW is important to energy policy in mitigating air pollution in China and other developing nations. However, the nonlinearity of atmospheric processes renders any firm conclusion hard to come by. Here we report the results of a 3-y, multiparameter sampling campaign in combination with atmospheric chemical model to examine the role of CDW.

Significance

Water vapor emitted from anthropogenic combustion for winter heating in northern China may exacerbate air pollution. This hypothesis is of considerable scientific and environmental interest. We conducted a multiyear sampling campaign of air vapor isotope compositions and associated atmospheric data from the city of Xi'an, located in an enclosed basin in northwestern China. We found that the fraction of combustion-derived water vapor increases with increasing relative humidity and with the concentration of particulate matter with an aerodynamic diameter less than 2.5 μm in polluted conditions based on field observation, isotopic analysis, and numerical simulation. Our results demonstrated that combustion-derived water is nontrivial when considering energy policy for improving air quality.

Author contributions: W.L., J.C., and Z.A. designed research; M.X., W.L., G.L., J.C., H.B., and Z.A. performed research; M.X., W.L., Xia Li, Q.W., J.T., Xiaofei Li, X.T., G.L., J.C., H.B., and Z.A. analyzed data; and M.X., W.L., Xia Li, W.Z., Q.W., J.T., Xiaofei Li, X.T., G.L., J.C., H.B., and Z.A. wrote the paper.

Reviewers: G.J.B., University of Utah; and X.Y., Fudan University.

The authors declare no competing interest.

See online for related content such as Commentaries.

[1]To whom correspondence may be addressed. Email: jjcao@ieecas.cn, bao@lsu.edu, or anzs@loess.llqg.ac.cn.

This article contains supporting information online at https://www.pnas.org/lookup/suppl/doi:10.1073/pnas.1922840117/-/DCSupplemental.

First published December 15, 2020.

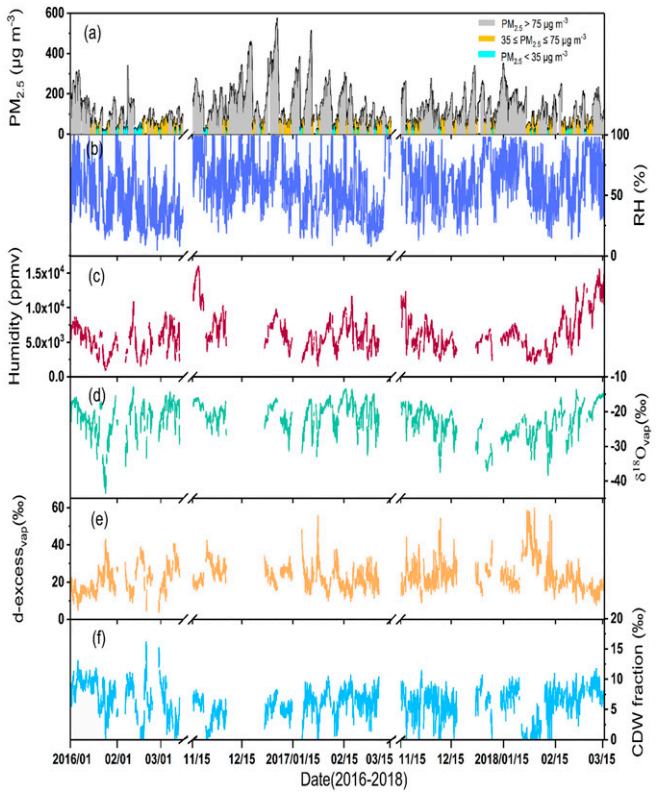

Fig. 1. Time-series variations in Xi'an during 2016–2018 heating seasons: [$PM_{2.5}$] (*A*); relative humidity (*B*); humidity (*C*); $\delta^{18}O_{vap}$ (vapor $\delta^{18}O$) (*D*); $d\text{-excess}_{vap}$ (vapor d-excess) (*E*); calculated fractions for CDW (*F*).

Results and Discussion

CDW Isotopic Compositions and Fraction in Total Air Moisture. To examine the impact of CDW on air pollution, we must first quantify the fraction of CDW in an airshed. CDW has a set of characteristic δD and $\delta^{18}O$ values that are locally specific and can be estimated based on energy inventory in a region. Here we conducted a winter-season atmospheric physical and chemical observational campaign from the year 2016–2018 in Xi'an, a densely populated city in the Guanzhong Basin (GZB) in northwestern China (*SI Appendix*, Fig. S1). The GZB is surrounded by the Loess Plateau to the north and Qinling Mountains to the south with a narrow opening to the east, a topography resulting in frequently stagnant air and heavy haze events in winter. Near-surface atmospheric water vapor δD and $\delta^{18}O$ values were continuously measured and compiled with rainy days excluded. End-member δD and $\delta^{18}O$ of fossil fuels such as coal, natural gas, and gasoline were individually determined experimentally (*SI Appendix*, *Materials and Methods*), and a weighted end-member isotope composition for CDW was obtained by using energy inventory in Xi'an Municipal Bureau of Statistics (21). A statistical analysis of the interrelationships among the fraction of CDW in total air moisture, [$PM_{2.5}$] range, RH, SO_2 concentrations ([SO_2]) range, and NO_2 concentrations ([NO_2]) range were conducted. A 19-d heavy haze event from Dec. 27, 2015 to Jan. 15, 2016 was then modeled using the Weather Research and Forecasting (WRF)-Chem model to examine the impact of SO_2, NO_2, and the added CDW on $PM_{2.5}$ formation.

Time-series data revealed that atmospheric RH was higher than nonhaze periods during all of the 40 observed heavy haze events when the [$PM_{2.5}$] were higher than 75 μg m^{-3} for more than 24 h (Fig. 1). The more positive $\delta^{18}O$ values (up to −15‰) for water vapor occurred during the periods of heavy haze events (*SI Appendix*, Fig. S2*A*). Overall, the water vapor $d\text{-excess}_{vap}$ (defined as $d\text{-excess}_{vap} = \delta^2H_{vap} - 8*\delta^{18}O_{vap}$) in Xi'an became less positive with a minimum value of 3‰ at higher [$PM_{2.5}$] (Fig. 1 and *SI Appendix*, Fig. S2*B*). By measuring the δD and $\delta^{18}O$ of CDW for individual fuels of different exhaust types, we obtained a weighted δD and $\delta^{18}O$ values for CDW in Xi'an (Fig. 2) at −134.4‰ and 9.0‰, respectively (*SI Appendix*, *Materials and Methods*).

We consider atmospheric water vapor as the sum of natural water (NW) and CDW. Recent studies have demonstrated that a high $d\text{-excess}_{vap}$ is generally observed in airshed with good dispersion condition (20, 22, 23) and low RH (24, 25). Thus, the δD and $\delta^{18}O$ of NW from such atmospheric conditions define a background line in δD-$\delta^{18}O$ space for those of polluted days to compare to. This background line was determined using an expectation-maximization algorithm for Gaussian mixture models which is known to be effective in separating individual components from a multicomponent mixture (26) (*SI Appendix*, *Materials and Methods*). To calculate the CDW fraction, we use the two-endmember mixing equation (20):

$$d_{vap} = d_{CDW}X + d_{NW}(1\text{-}X), \quad [1]$$

where d_{vap} is the observed water vapor d-excess (point C in *SI Appendix*, Fig. S3), d_{CDW} is Xi'an's weighted CDW d-excess (point B in *SI Appendix*, Fig. S3), d_{NW} is d-excess of NW (point A in *SI Appendix*, Fig. S3, the intersection of the extended BC line with the background line), and X is the fraction of CDW (the length ratio of line AC over line AB, *SI Appendix*, Fig. S3). For those points to the left side of the background line, we consider their CDW fraction as zero. The position of the background line determines the CDW fraction. There are uncertainties, including condensation due to adiabatic lifting (27), kinetic effects due to evaporation (28), and mixing of air masses (29), that are associated with the determination of the background line. We compared three independent methods: 1) using an optimized smooth function on observed time-series d-excess data (20), 2)

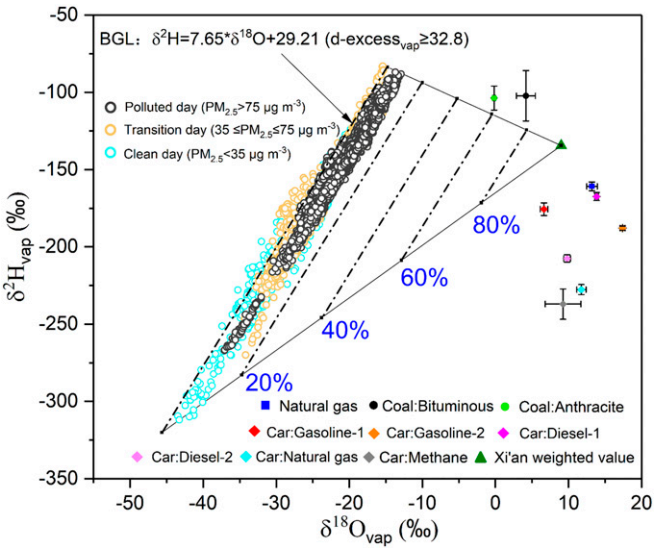

Fig. 2. Surface air vapor isotopic composition (δ^2H_{vap} and $\delta^{18}O_{vap}$) and different fossil fuel CDW vapor isotopic composition in Xi'an. BGL represents the background line of vapor isotopic composition calculated according to a Gaussian mixing model. The circles of three different colors represent different ranges of [$PM_{2.5}$]. The solid green triangle is Xi'an's weighted isotope composition of CDW calculated according to energy inventory. The dashed lines represent CDW fraction in total moisture. Uncertainties of the data are marked or smaller than the symbol sizes.

using measured d-excess data prior to the rising of air pollutants (23, 27), and 3) using an expectation-maximization algorithm for Gaussian mixture models in this study. We found that the Gaussian mixture models gave CDW fractions higher than those in Gorski et al. (20), but nearly identical to those in Fiorella et al. (23, 27) (*SI Appendix*, Fig. S4). The average contribution of CDW is 6.2% in Xi'an, and the highest fraction is found to be 16.2% of the total surface air moisture.

The Xi'an water vapor isotope data display a similar δD-$\delta^{18}O$ pattern as that observed in Salt Lake City (20). This may be attributed to the similar enclosed topography of the two sites, where CDW is kept under often stagnant meteorological conditions. Occurrences of winter haze in Xi'an provide us an opportunity to explore the relationship between CDW fraction and its potential effect on secondary $PM_{2.5}$ formation by using water vapor isotopes.

Relations among [SO_2], [NO_2], RH, CDW, and [$PM_{2.5}$]. We plotted the ranges of [SO_2] and [NO_2] with those of RH and [$PM_{2.5}$] for the three heating seasons (Fig. 3 and *SI Appendix*, Table S1). The data show that when the [SO_2] are less than 15 μg m^{-3} and RH is lower than 60%, the [$PM_{2.5}$] remains below 35 μg m^{-3}. This is also the case as long as the [NO_2] are less than 20 μg m^{-3}. Severe haze events with [$PM_{2.5}$] higher than 150 μg m^{-3} occur only when RH is higher than 40% while in the same time [SO_2] are higher than 30 μg m^{-3} or [NO_2] higher than 60 μg m^{-3}. The higher the RH is, the higher is the CDW fraction in total moisture during periods of [$PM_{2.5}$] rising (*SI Appendix*, Fig. S5). Overall, the CDW fraction increases from an average of 5.5% to 6.5% when the RH increases from 20–40% to 60–80%, respectively, which also means that in absolute quantity, the increase of CDW is significant in air with high RH (Fig. 3).

The rapid increase of [$PM_{2.5}$] is controlled by many factors, such as the seasonally enhanced emissions of primary pollutants from residential heating in winter (e.g., coal combustion, natural gas burning, and biomass burning) (30), the fast growth of secondary aerosols (31, 32), and unfavorable meteorological conditions (15, 33). For the formation of secondary aerosols, previous studies have noticed the enhanced reaction rates at high RH level (32, 34–36). Here, considering the contribution of CDW to RH, we used the WRF-Chem model to evaluate CDW's role in $PM_{2.5}$ formation during a persistent and heavy haze episode in the GZB (*SI Appendix*, Fig. S6).

Modeling. The WRF-Chem model performed well in simulating particulate pollution in China (17, 37, 38), and reasonably reproduced the observed temporal variations and spatial distributions of [$PM_{2.5}$], [O_3], [NO_2], and [SO_2] in the GZB and Xi'an city (*SI Appendix*, Fig. S7) during the simulation period in the present study. The results show that the addition of CDW generally increases [$PM_{2.5}$] and can be up to 16.6 μg m^{-3} or an additional 8% in the GZB (Fig. 4 *A* and *B*), and 20.0 μg m^{-3} or 10% in Xi'an airshed (*SI Appendix*, Fig. S8 *A* and *B*). On average, CDW promoted additional $PM_{2.5}$ formation by 2.8% (equivalent to 4.6 μg m^{-3}) in the GZB and 3.4% (equivalent to 6.0 μg m^{-3}) in Xi'an and its surrounding areas during the 19-d period of heavy particulate pollution when the average [$PM_{2.5}$] were at 164.1 μg m^{-3} in the GZB and 177.3 μg m^{-3} in Xi'an. Approximately 86% of the enhanced $PM_{2.5}$ from CDW is contributed by secondary aerosols, in which the contributions from secondary organic and inorganic aerosols are 44% and 42%, respectively. The rest of the $PM_{2.5}$ enhancement is mainly contributed by the aerosol-radiation feedback induced by an increase in aerosol liquid water.

The severe and persistent particulate pollution in the GZB could be attributed to a synergy of massive anthropogenic emissions and unfavorable synoptic conditions related to the topography (7, 39–41). We further conducted a sensitivity simulation considering only the local anthropogenic emissions in the GZB in the emission inventory (mainly including agriculture, industry, power, residential, and transportation sources) used in the WRF-Chem model to evaluate the contribution of CDW to the $PM_{2.5}$ level from local anthropogenic emissions. On average the CDW-enhanced [$PM_{2.5}$] accounts for about 5.1% of the average [$PM_{2.5}$] (91.0 μg m^{-3}) and up to 18.2% from the local anthropogenic emissions in the GZB. Considering that [$PM_{2.5}$] control target for the fall and winter of 2019 (a 6-mo period) in Xi'an was a reduction of 2 μg m^{-3}, this additional increase of [$PM_{2.5}$] would likely counteract many of the implemented [$PM_{2.5}$] reduction efforts.

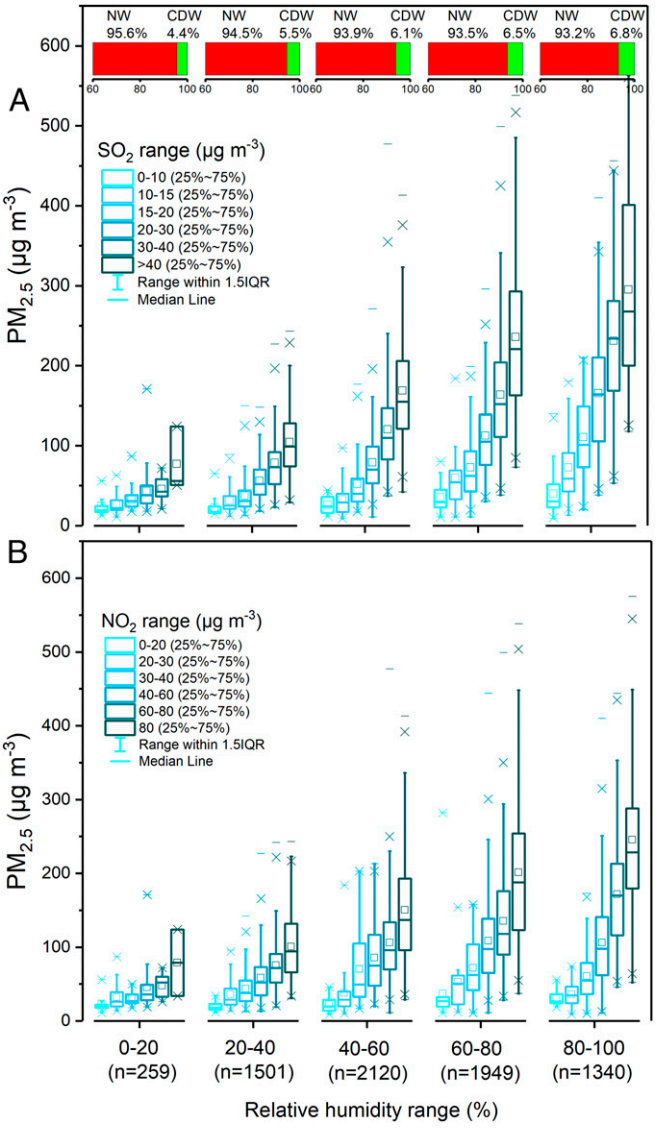

Fig. 3. The [$PM_{2.5}$] at different RH and SO_2 (concentration) ranges (*A*) and at different RH and NO_2 (concentration) ranges (*B*); the bar graphs in the top panel represent percentage contributions of NW and CDW. The blue color shades represent the SO_2 and NO_2 ranges from 0 to above 40 μg m^{-3} and from 0 to above 80 μg m^{-3}, respectively. The hollow squares inside the vertically elongated boxes are the average [$PM_{2.5}$]; the center line within a box is the median of the [$PM_{2.5}$] dataset; the upper and lower edges of the box are the 25% and 75% of the [$PM_{2.5}$] dataset; the ends of the lines extending from the interquartile range (IQR) represent the extreme values within 1.5× the IQR; the cross and the minus signs represent outliers that are at a greater distance from the median than 1.5× the IQR (see *SI Appendix, Materials and Methods* for statistical test).

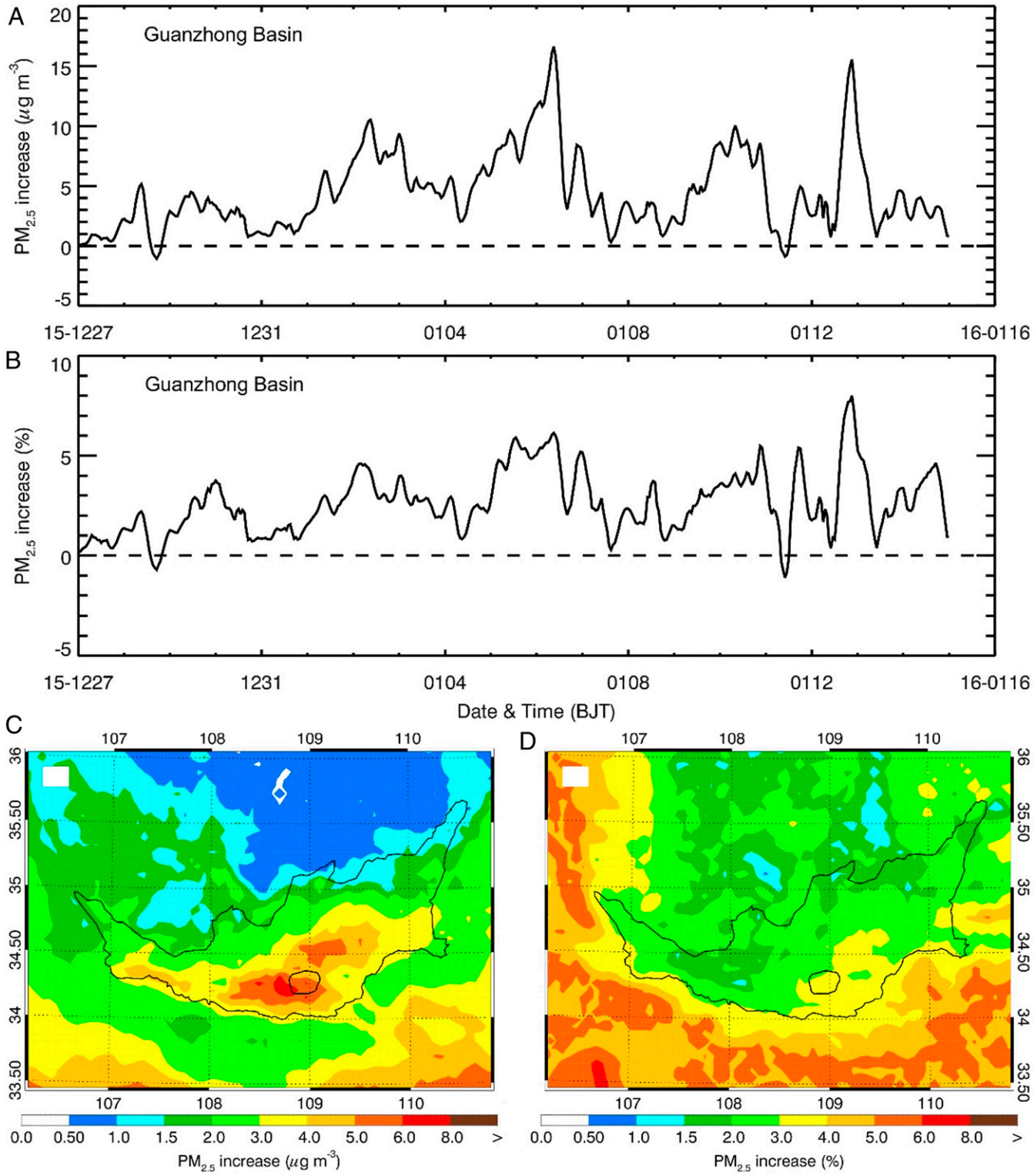

Fig. 4. Effects of CDW on near-surface [$PM_{2.5}$] in the GZB. (*A* and *B*) Diurnal profiles of average [$PM_{2.5}$] increase in GZB from 00:00 (Beijing time, BJT) Dec. 27, 2015 to 00:00 BJT Jan. 15, 2016 in μg/m^3 or in %; (*C* and *D*) Spatial distribution of average [$PM_{2.5}$] increase during the simulation period in μg m^3 or in %. The outer black line outlines the location of GZB, and the inner black line outlines the urban area of Xi'an.

To quantify the effectiveness of curtailing the formation of secondary aerosols by reducing NO_2 or SO_2 emissions or CDW, we have conducted a sensitivity test using a typical polluted day as our base case ([SO_2] = 47.9, [NO_2] = 70.8, [$PM_{2.5}$] = 164.1, all in μg m^{-3}, and RH = 58.9%) (*SI Appendix*, Table S2 *A* and *B*). When both RH and [SO_2] are reduced to 53.1% and 10.3 μg m^{-3}, respectively, the [$PM_{2.5}$] decreases by 8.0 μg m^{-3}. When both RH and [NO_2] are dropped to 53.1% and 19.7 μg m^{-3}, the [$PM_{2.5}$] increases, however, by 0.9 μg m^{-3} comparing with the RH reduction-only scenario. When both RH, [SO_2], and [NO_2]

are dropped to 53.1%, 8.9 μg m^{-3}, and 19.6 μg m^{-3}, respectively, the [$PM_{2.5}$] decreases by 20.2 μg m^{-3}. Note that the model predicts a 4.6 μg m^{-3} reduction of [$PM_{2.5}$] in the GZB if we subtract from the model the CDW contribution which is on average ∼10% of the overall RH during the 19-d period in early 2016 (*SI Appendix*, Fig. S9). This level of $PM_{2.5}$ reduction by eliminating CDW is not overwhelming but still significant when comparing to the effort that would be required to achieve the same reduction by reducing [SO_2] and/or [NO_2].

The positive feedback mechanism between RH and $PM_{2.5}$ growth rate has been proposed previously (15, 42). Briefly, the RH increases and induces the formation of secondary particulate matter through aqueous reactions in a shallow PBL condition. This in turn enhances the formation of particulate matter and results in solar dimming, which then limits the PBL height. Wu et al. (17) estimated that the average contribution of the water vapor (including natural and anthropogenic factors) to the near-surface increased [$PM_{2.5}$] is 17.5%, indicating its importance. Using water vapor isotope data, we have further differentiated the $PM_{2.5}$ contribution between anthropogenic factor and natural water vapor effect. Our results suggest that CDW promotes additional $PM_{2.5}$ formation, being consistent with the previously proposed positive-feedback hypothesis. A long-term observational dataset in combination with modeling is required to further quantify CDW's positive-feedback effect on secondary aerosol formation.

Policy Implications. The Chinese government issued a series of counterpollution measures in which the "coal-to-gas" campaign was widely implemented in household heating in the North China Plain, aiming at improving the air quality (43, 44). The natural gas combustion can produce 3× more water vapor than coal burning. This number is based on mean calorific capacities of coal and natural gas and therefore the quantity needed to generate 1 megawatt-hour equivalent energy (*SI Appendix, Materials and Methods*). As demonstrated by our study, CDW in urban PBL could promote additional formation of secondary aerosols and therefore exacerbate air quality. Thus, while the enhancing effect of CDW on $PM_{2.5}$ formation needs to be further quantified in additional urban areas, caution is warranted in implementing the coal-to-gas switch for household in North China Plain and other areas.

Materials and Methods

A Cavity Ring-Down Spectroscopy analyzer (model Picarro-L2130i, Picarro, Inc.) was used for δD and $\delta^{18}O$ measurement. A recommended dual mode (45) was followed. The humidity effect was corrected by a humidity-isotope calibration response function (46). The data were calibrated to the VSMOW-GISP scale with six known standards runs at regular intervals (47, 48). Large chambers up to the size of a shipping container were used to experimentally determine the δD and $\delta^{18}O$ of CDW generated by industry-scaled natural gas and coal burning. Those from diverse car exhausts were measured via a pipe on a transmission device at Xi'an Automobile Testing Center. Weighted isotopic compositions were calculated using energy inventory obtained from Xi'an Municipal Bureau of Statistics (21). To obtain a set of background of d-$excess_{vap}$ values, we followed Steen-Larsen et al. (28) and performed a cluster analysis using an expectation-maximization algorithm for Gaussian mixture models (26). The results displayed a distinct cluster with a mean d-$excess_{vap}$ of 19.7‰ and an SD (σ) of 4.38‰, and a second cluster centered around 28‰ with σ = 8.35‰. We arbitrarily defined a high d-$excess_{vap}$ value being +3σ higher than the mean d-$excess_{vap}$ value of the main cluster, i.e., at 32.8‰. A background $\delta^{18}O_{vap}$ $-\delta^{2}H_{vap}$ line with d-$excess_{vap}$ greater than 32.8‰ was constructed by linear regression.

Hourly concentration data of atmospheric gases, such as SO_2, NO_2, CO, O_3, and $PM_{2.5}$, and the meteorological data including temperature, RH, and amount of precipitation in Xi'an were downloaded from government websites of https://www.aqistudy.cn/ and http://www.weather.com.cn/, respectively. In determining the impact of [SO_2], [NO_2], and RH on [$PM_{2.5}$], we compared the significant differences of [$PM_{2.5}$] with the [SO_2] and [NO_2] categories at different RH ranges by using one-way ANOVA tests at $P = 0.01$ level (*SI Appendix*, Table S3 *A* and *B*).

The WRF-Chem model modified by Li et al. (49–52) was used to simulate a 19-d persistent and heavy haze episode from late December 2015 to January 2016. The WRF-Chem model adopts one grid with a horizontal resolution of 6 km centered at 34.25°N and 109.0°E (*SI Appendix*, Fig. S6), and 35 sigma vertical levels with a stretched vertical grid with spacing ranging from 30 m near the surface, to 500 m at 2.5 km and 1 km above 14 km, and the grid cells used for the domain are 150 × 150. The physical parametrizations employed in the model are listed in *SI Appendix*, Table S4. The contribution of CDW to the [$PM_{2.5}$] was quantitatively determined by comparing the model-simulated 19-d case (which broadly fits the observation) with a corresponding case in which the CDW input was arbitrarily set at zero in the GZB.

Data Availability. All data are included in the article, *SI Appendix*, or available at the East Asian Paleoenvironmental Science Database, http://paleodata.ieecas.cn/FrmDataInfo_EN.aspx?id=e38d7bfb-067a-4cbc-b42d-37216594f371.

ACKNOWLEDGMENTS. Financial support comes from the Strategic Priority Research Program of Chinese Academy of Sciences Grant (XDB40000000), National Research Program for Key Issues in Air Pollution Control (China) Grant (DQGG0105), National Atmospheric Research Program (China) Grant (2017YFC0212200), Key Projects of Chinese Academy of Sciences Grant (ZDRW-ZS-2017-6), State Key Laboratory of Loess and Quaternary Geology Grant (SKLLQGZD1701), China scholarship council, and Charles Jones Professorship fund (H.B.).

1. J. Lelieveld, J. S. Evans, M. Fnais, D. Giannadaki, A. Pozzer, The contribution of outdoor air pollution sources to premature mortality on a global scale. *Nature* **525**, 367–371 (2015).
2. F. Laden, J. Schwartz, F. E. Speizer, D. W. Dockery, Reduction in fine particulate air pollution and mortality: Extended follow-up of the Harvard Six Cities study. *Am. J. Respir. Crit. Care Med.* **173**, 667–672 (2006).
3. J. Watson *et al.*; National Academy of Engineering; National Research Council; Chinese Academy of Sciences, *Energy futures and urban air pollution: Challenges for China and the United States* (National Academies Press, Washington, DC, 2008), pp. 1–366.
4. J. Cao, China-US cooperation to advance nuclear power. *Science* **6299**, 547–548 (2016).
5. UN Environment, *A Review of 20 years' Air Pollution Control in Beijing* (United Nations Environment Programme, Nairobi, Kenya, 2019), pp. 1–64.
6. Z. Ma, R. Liu, Y. Liu, J. Bi, Effects of air pollution control policies on PM 2.5 pollution improvement in China from 2005 to 2017: A satellite-based perspective. *Atmos. Chem. Phys.* **19**, 6861–6877 (2019).
7. Z. An *et al.*, Severe haze in northern China: A synergy of anthropogenic emissions and atmospheric processes. *Proc. Natl. Acad. Sci. U.S.A.* **116**, 8657–8666 (2019).
8. Nature Geoscience, Cleaner air for China. *Nat. Geosci.* **12**, 497 (2019).
9. B. Zhao *et al.*, Change in household fuels dominates the decrease in $PM_{2.5}$ exposure and premature mortality in China in 2005-2015. *Proc. Natl. Acad. Sci. U.S.A.* **115**, 12401–12406 (2018).
10. Ministry of Environmental Protection of China, Work plan for air pollution control in Beijing-Tianjin-Hebei and its surrounding areas in 2017 (Ministry of Environmental Protection of China, Beijing). (2017). dqhj.mee.gov.cn/dtxx/201703/t20170323_408663.shtml. Accessed 14 February 2020).
11. National Development and Reform Commission of China, Work plan for clean heating in winter in northern China (2017–2021) (National Development and Reform Commission of China, Beijing). (2017). http://www.gov.cn/xinwen/2017-12/20/content_5248855.htm. Accessed 14 February 2020.
12. A. Miyamoto, C. Ishiguro, *The outlook for natural gas and LNG in China in the war against air pollution* (Oxford Institute for Energy Studies, England, 2018), pp. 1–53.
13. S. Xu, J. Ge, Sustainable shifting from coal to gas in North China: An analysis of resident satisfaction. *Energy Policy* **138**, 111296 (2020).
14. Z. Wu *et al.*, Interactions between water vapor and atmospheric aerosols have key roles in air quality and climate change. *Natl. Sci. Rev.* **5**, 452–454 (2018).
15. X. Tie *et al.*, Severe pollution in China amplified by atmospheric moisture. *Sci. Rep.* **7**, 15760 (2017).
16. T. Petäjä *et al.*, Enhanced air pollution via aerosol-boundary layer feedback in China. *Sci. Rep.* **6**, 18998 (2016).
17. J. Wu *et al.*, Is water vapor a key player of the wintertime haze in North China Plain? *Atmos. Chem. Phys.* **19**, 8721–8739 (2019).
18. J. Galewsky *et al.*, Stable isotopes in atmospheric water vapor and applications to the hydrologic cycle. *Rev. Geophys.* **54**, 1–57 (2016).
19. J. Worden, D. Noone, K. Bowman; Tropospheric Emission Spectrometer Science Team and Data contributors, Importance of rain evaporation and continental convection in the tropical water cycle. *Nature* **445**, 528–532 (2007).
20. G. Gorski *et al.*, Vapor hydrogen and oxygen isotopes reflect water of combustion in the urban atmosphere. *Proc. Natl. Acad. Sci. U.S.A.* **112**, 3247–3252 (2015).
21. Xi'an Municipal Bureau of Statistics, *Xian Statistical Yearbook 2018*, M. Zhang, X. Wang, Eds. (China Statistics Press, Beijing, 2018), pp. 461–477.

22. O. E. Salmon *et al*., Urban emissions of water vapor in winter. *J. Geophys. Res. Atmos.* **122**, 9467–9484 (2017).
23. R. P. Fiorella, R. Bares, J. C. Lin, J. R. Ehleringer, G. J. Bowen, Detection and variability of combustion-derived vapor in an urban basin. *Atmos. Chem. Phys.* **18**, 8529–8547 (2018).
24. J. Galewsky, K. Samuels-Crow, Summertime moisture transport to the southern South American Altiplano: Constraints from in situ measurements of water vapor isotopic composition. *J. Clim.* **28**, 2635–2649 (2015).
25. K. E. Samuels-Crow, G. Joseph, Deuterium excess in subtropical free troposphere water vapor: Continuous measurements from the Chajnantor Plateau, northern Chile. *Geophys. Res. Lett.* **41**, 8652–8659 (2014).
26. T. K. Moon, The expectation-maximization algorithm. *IEEE Signal Process. Mag.* **13**, 47–60 (1996).
27. R. P. Fiorella, R. Bares, J. C. Lin, G. J. Bowen, Wintertime decoupling of urban valley and rural ridge hydrological processes revealed through stable water isotopes. *Atmos. Environ.* **213**, 337–348 (2019).
28. Z. Wei, X. Lee, The utility of near-surface water vapor deuterium excess as an indicator of atmospheric moisture source. *J. Hydrol. (Amst.)* **577**, 123923 (2019).
29. T. J. Griffis *et al*., Investigating the source, transport, and isotope composition of water vapor in the planetary boundary layer. *Atmos. Chem. Phys.* **16**, 5139–5157 (2016).
30. J. Liu *et al*., Air pollutant emissions from Chinese households: A major and underappreciated ambient pollution source. *Proc. Natl. Acad. Sci. U.S.A.* **113**, 7756–7761 (2016).
31. R. J. Huang *et al*., High secondary aerosol contribution to particulate pollution during haze events in China. *Nature* **514**, 218–222 (2014).
32. R. J. Huang *et al*., Primary emissions versus secondary formation of fine particulate matter in the most polluted city (Shijiazhuang) in North China. *Atmos. Chem. Phys.* **19**, 2283–2298 (2019).
33. R. Zhang *et al*., Formation of urban fine particulate matter. *Chem. Rev.* **115**, 3803–3855 (2015).
34. M. Elser *et al*., New insights into PM2.5 chemical composition and sources in two major cities in China during extreme haze events using aerosol mass spectrometry. *Atmos. Chem. Phys. Discuss.* **15**, 30127–30174 (2015).
35. G. Li *et al*., A possible pathway for rapid growth of sulfate during haze days in China. *Atmos. Chem. Phys.* **17**, 1–43 (2017).
36. G. Wang *et al*., Persistent sulfate formation from London Fog to Chinese haze. *Proc. Natl. Acad. Sci. U.S.A.* **113**, 13630–13635 (2016).
37. J. Wu *et al*., Aerosol-photolysis interaction reduces particulate matter during wintertime haze events. *Proc. Natl. Acad. Sci. U.S.A.* **117**, 9755–9761 (2020).
38. T. Le *et al*., Unexpected air pollution with marked emission reductions during the COVID-19 outbreak in China. *Science* eabb7431 (2020).
39. N. Bei, Bs. Xiao, N. Meng, T. Feng, Critical role of meteorological conditions in a persistent haze episode in the Guanzhong basin, China. *Sci. Total Environ.* **550**, 273–284 (2016).
40. N. Bei *et al*., Typical synoptic situations and their impacts on the wintertime air pollution in the Guanzhong basin, China. *Atmos. Chem. Phys.* **16**, 7373–7387 (2016).
41. X. Long *et al*., Impact of crop field burning and mountains on heavy haze in the north China plain: A case study. *Atmos. Chem. Phys.* **16**, 9675–9691 (2016).
42. Q. Liu *et al*., New positive feedback mechanism between boundary layer meteorology and secondary aerosol formation during severe haze events. *Sci. Rep.* **8**, 6095 (2018).
43. K. Dong *et al*., Environmental Kuznets curve for PM2.5 emissions in Beijing, China: What role can natural gas consumption play? *Ecol. Indic.* **93**, 591–601 (2018).
44. Y. Xue *et al*., Spatio-temporal variations of multiple primary air pollutants emissions in Beijing of China, 2006-2015. *Atmosphere (Basel)* **10**, 2006–2015 (2019).
45. M. Benetti *et al*., Deuterium excess in marine water vapor: Dependency on relative humidity and surface wind speed during evaporation. *J. Geophys. Res. Atmos.* **119**, 584–593 (2014).
46. D. Noone *et al*., Determining water sources in the boundary layer from tall tower profiles of water vapor and surface water isotope ratios after a snowstorm in Colorado. *Atmos. Chem. Phys.* **13**, 1607–1623 (2013).
47. H. C. Steen-Larsen *et al*., Continuous monitoring of summer surface water vapor isotopic composition above the Greenland Ice Sheet. *Atmos. Chem. Phys.* **13**, 4815–4828 (2013).
48. F. Aemisegger *et al*., Measuring variations of δ 18O and δ 2H in atmospheric water vapour using two commercial laser-based spectrometers: An instrument characterisation study. *Atmos. Meas. Tech.* **5**, 1491–1511 (2012).
49. G. Li, N. Bei, X. Tie, L. T. Molina, Aerosol effects on the photochemistry in Mexico City during MCMA-2006/MILAGRO campaign. *Atmos. Chem. Phys.* **11**, 5169–5182 (2011).
50. G. Li, W. Lei, N. Bei, L. T. Molina, Contribution of garbage burning to chloride and PM 2.5 in Mexico City. *Atmos. Chem. Phys.* **12**, 8751–8761 (2012).
51. G. Li *et al*., Impacts of HONO sources on the photochemistry in Mexico city during the MCMA-2006/MILAGO campaign. *Atmos. Chem. Phys.* **10**, 6551–6567 (2010).
52. G. Li *et al*., Simulations of organic aerosol concentrations in Mexico City using the WRF-CHEM model during the MCMA-2006/MILAGRO campaign. *Atmos. Chem. Phys.* **11**, 3789–3809 (2011).